

Notice: This material may be protected by Copyright Law
(Title 17 U.S. Code)



ILL record updated to IN PROCESS
Record 28 of 45

lg

Record 30 of 45
NOV 20 2001

ILL pe
CAN YOU SUPPLY ? YES NO COND FUTUREDATE
: ILL: 2721010 : Borrower: MNU : RegDate: 20011119 : NeedBefore: 20011219
: Status: IN PROCESS 20011119 : RecDate: NA : RenewalReq:
: OCLC: 6887276 : Source: OCLCILL : DueDate: : NewDueDate:
: Lender: *UPM UPM, NUI, EYM
: CALLNO: *QA 759 .6 .E4*
: TITLE: Electromagnetics.
: IMPRINT: Washington, D.C. : Hemisphere Pub. Corp., c1981-
: ARTICLE: Resit Sendag and A. Hamit Serbest. "Scattering at the Junction
formed by a PEC half-plane and half-plane.."
: VOL: 21 : NO: 5 : DATE: 2001
: VERIFIED: OCLC ISSN: 0272-6343
: PATRON: Sendag, Resit, grad/me
: PAGES: 415-435 *f*

ONLY 1/2 x 11

SHIP TO: ILL
CIC
110 Wilson Library
University of Minnesota
309 19th Avenue South
Minneapolis, MN 55455

8
:BILL TO: same/ ARL, CIC, RLG: :MAXCOST: :COPYRT COMPLIANCE: CCG
:SHIP VIA: Library Rate
:FAX: 612-626-7585
:E-MAIL: wilsill@tc.umn.edu / ARIEL: 160.94.230.141
:BILLING NOTES: FEIN #41-6007513
:AFFILIATION: PALS Libraries ship via MINITEX.
:LENDING CHARGES: :SHIPPED: :SHIP INSURANCE:
:LENDING RESTRICTIONS:
:LENDING NOTES:
:RETURN TO:
:RETURN VIA:



Scattering at the Junction Formed by a PEC Half-Plane and a Half-Plane with Anisotropic Conductivity

REŞİT ŞENDAĞ

A. HAMİT SERBEST

Department of Electrical and Electronics Engineering
Faculty of Engineering and Architecture
Çukurova University
Adana, Turkey

In this study, scattering of plane electromagnetic waves at the junction formed by a PEC half-plane and a half-plane with anisotropic conductivity is investigated. By using a Fourier transform technique, the problem is formulated into a matrix Wiener-Hopf system, and a rigorous solution is obtained. Also, to show the effect of planar physical discontinuity explicitly, four different special cases are considered where the problems are reduced into pairs of simultaneous Wiener-Hopf equations. They are decoupled via polynomial transformations and solved through the standard procedure. The diffracted fields are expressed in a form suitable for GTD applications.

Keywords diffraction, anisotropic conductivity, plane discontinuity

Introduction

The diffraction of electromagnetic waves by a half-plane or a plane discontinuity composed of two half-planes with different physical properties has been studied by many authors, and a short summary of the subject was given by Serbest (1997). In some of these works, the electromagnetic property of an imperfectly conducting slab is specified by its scalar resistivity $R = (1/\sigma t)$ with σ being the conductivity and t being the thickness, which is assumed to be small compared with the wavelength. In the most general case, the surface resistivity may be anisotropic supporting electric current sheets in directions parallel to both normal and tangential axes of the plane (Senior, 1978). For such a plane located at $y = 0$, a constant resistivity tensor can be written in the following dyadic form:

$$\overline{\overline{R}} = R_1 \hat{x} \hat{x} + R_2 \hat{z} \hat{z}. \quad (1)$$

Received 20 August 2000, accepted 21 January 2001.

The authors are thankful to the reviewers for their comments, which helped to improve the paper.

Address correspondence to A. Hamit Serbest, Department of Electrical and Electronic Engineering, Faculty of Engineering and Architecture, Çukurova University, Adana, Turkey, 01330. E-mail: serbest@cu.edu.tr

where \hat{x} and \hat{z} denote the unit vectors in cartesian coordinate system. Here, R_1 and R_2 represent

$$R_1 = (1/\sigma_x t) \quad \text{and} \quad R_2 = (1/\sigma_z t) \quad (2)$$

with σ_x and σ_z being the conductivities in the x and z directions, respectively.

Anisotropy is a characteristic and interesting feature of materials and it should necessarily be taken into account in order to form a realistic mathematical model of a matter. But, due to the mathematical complexity that is encountered with these realistic models, the number of studies that have appeared in the open literature are relatively few and the ones that have appeared correspond to some special cases. One of the earliest studies about an anisotropically conducting surface was presented by Hurd (1960), in which where he mentioned that the first two papers in this subject were due to Toraldo di Francia (1956) and Karp (1957). In these papers, the surface was taken as unidirectionally conducting, which has infinite and zero conductivities along the axes perpendicular to each other. This is a special case of the anisotropic conductance. An impedance-type anisotropy was considered for the half-plane case by Hurd and Lüneburg (1985). and Serbest, Büyükaksoy, and Uzgoren (1991) studied the discontinuity formed by two anisotropic impedance half-planes assuming the plane to be PEC in one direction and with impedance discontinuity in the other direction. Büyükaksoy, Serbest, and Kara (1996) also considered the half-plane with anisotropic conductivity. Some practically more involved anisotropic half-planes were considered by Rozov and Tretyakov (1981), (1984), and Rozov and Sochava (1991).

In this work, scattering of plane electromagnetic waves at the junction formed by a PEC half-plane and a half-plane with anisotropic conductivity is considered for the oblique incidence case. This junction will display the effects of the conductance discontinuity mechanism along both axes of the plane. The structure of the half-plane with anisotropic conductivity is simulated by standard resistive boundary conditions, and the problem is formulated by the Fourier transform technique. The formal solution is derived for the diffraction problem by employing the well-known Daniele–Khrapkov method (Büyükaksoy, Serbest, 1993). While an exact closed-form solution is obtained by factorizing a 2×2 Wiener–Hopf matrix, not only that is it quite complicated algebraically, but it also contains several transcendental functions need numerical consideration. Therefore, in the present investigation, the rigorous solution of the general problem is obtained in a formal manner that is too complicated to be used in engineering applications. This complexity is not too surprising for this type of anisotropy. In order to obtain some explicit analytical results with practical meaning, the mathematical model is simplified and four different special cases are examined to yield the effect of planar physical discontinuity. These problems correspond to the cases where R_1 and R_2 are taken as either zero or infinitely large. As known, the conductivity being zero or infinite means physically a perfectly conducting structure or a vanishing structure, respectively. All problems related to these special cases are formulated into pairs of simultaneous Wiener–Hopf equations that are decoupled via polynomial transformations and solved through the standard procedure. They show the diffraction mechanisms of the surfaces with conductance discontinuity along one direction, while in the other direction the structure is either infinite or semi-infinite and perfectly conducting.

Formulation of the Problem

The $y = 0$ plane, of which the negative half ($x < 0$) is a perfect electrical conductor (PEC) and the positive half ($x > 0$) has anisotropic conductivity (Figure 1), is illuminated by a plane electromagnetic wave given as

$$\vec{E}^i(x, y, z) = (A_x^i, A_y^i, A_z^i) e^{-ik \sin \theta_0 (x \cos \phi_0 + y \sin \phi_0)} e^{ikz \cos \theta_0} \quad (3)$$

Here $\vec{k} = (-k_x, -k_y, k_z)$, with $k_x = k \sin \theta_0 \cos \phi_0$, $k_y = k \sin \theta_0 \sin \phi_0$, and $k_z = k \cos \theta_0$ as the expressions of the propagation vector, and $\vec{k} \cdot \vec{A}^i = 0$ is satisfied. The time dependence is assumed to be $\exp(-i\omega t)$ and the z -dependence is assumed to be $\exp(ik_z z)$ of the incident field, which are common to all field quantities and will be suppressed throughout the analysis. In the above expressions θ_0 is the measure of obliquity, with $\theta_0 = \pi/2$ corresponding to the incidence in a plane perpendicular to the edge. k is the free-space wave number of the medium and ω is the angular frequency of the field. To make the incident and consequently the scattered field Fourier integrable with respect to x , the wave number is assumed to have a small positive imaginary part. Then the lossless case can be obtained by making $\text{Im}(k) \rightarrow 0$ in the final expressions.

The half-plane with anisotropic conductivity is assumed to have finite conductivity of R_1 in the x -direction and of R_2 in the z -direction, which can be characterized by the following general anisotropic resistivity conditions given by Senior (1978):

$$\hat{y} \times [\vec{E}(x, +0) - \vec{E}(x, -0)] = 0, \quad x > 0, \quad (4)$$

$$\hat{y} \times [\hat{y} \times \vec{E}(x, +0)] = -\vec{R} \hat{y} \cdot [\vec{H}(x, +0) - \vec{H}(x, -0)], \quad x > 0, \quad (5)$$

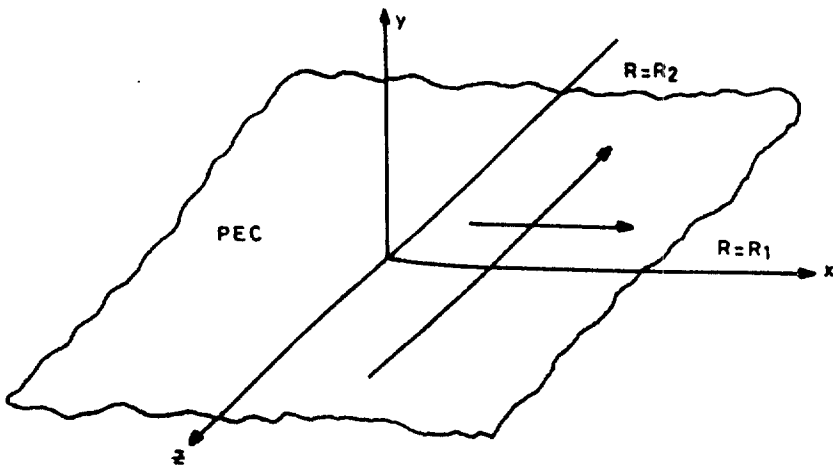


Figure 1. Geometry of the problem.

where $\bar{\bar{R}}$ is defined with (1) and \hat{y} is the unit vector directed along the y -axis. Here \bar{H} and \bar{H} denote the total fields, which are written as the sum of the incident and scattered field components

$$\bar{E}(\bar{H}) = \bar{E}^i(\bar{H}^i) + \bar{E}^s(\bar{H}^s)$$

for all y . As is known, to obtain the scattered fields, it is sufficient to consider the tangential components of the electric field. In order to be able to use the above boundary conditions, the tangential components of the magnetic field must also be known. These components can be derived easily from E_x^s and E_z^s via Maxwell's equations, and in order to determine the representation for E_y , divergence of the displacement vector will be used.

For E_x^s and E_z^s , which satisfy the reduced wave equation of the half-plane, one can assume the following integral representations:

$$E_z^s = \int_L A_{\pm}(\alpha) e^{-i\alpha x \pm i\Gamma(\alpha)y} d\alpha + E_z^r(E_z^i), \quad y \geq 0,$$

$$E_x^s = \int_L B_{\pm}(\alpha) e^{-i\alpha x \pm i\Gamma(\alpha)y} d\alpha + E_x^r(E_x^i), \quad y \geq 0,$$

where $\Gamma(\alpha) = \sqrt{N^2 - \alpha^2}$ with $N = \sqrt{k^2 - k_z^2} = k \sin \theta_0$. The square root function $\Gamma(\alpha)$ is defined in the complex α -plane cut as shown in Figure 2, such that $\Gamma(0) = N$.

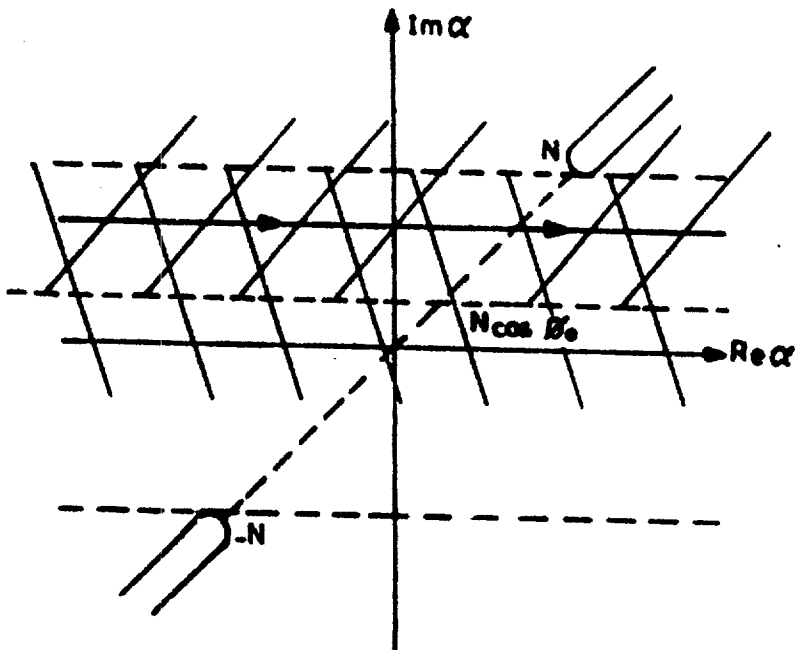


Figure 2. Complex α -plane and position of integration line L , where the regularity band is determined by $\text{Im}(\alpha) < \text{Im}(N)$ and $\text{Im}(\alpha) > \text{Im}(N \cos \phi_0)$.

The terms $E_x^{r,t}$ and $E_z^{r,t}$ are defined by

$$E_x^r(E_x^t) = R_x(T_x)A_x^i e^{-ik_x x \pm ik_y y}, \quad y \geq 0, \tag{8}$$

$$E_z^r(E_z^t) = R_z(T_z)A_z^i e^{-ik_x x \pm ik_y y}, \quad y \geq 0. \tag{9}$$

In (8) and (9), the (+) and (-) signs in the exponentials are used for the reflection terms in $y > 0$ half-space and for the transmission terms in $y < 0$ half-space, respectively. $R_x(T_x)$ and $R_z(T_z)$ denote the reflection (transmission) coefficients related to the x and z components of the electric field that would be reflected (transmitted) if the whole plane $y = 0$ were characterized by a constant surface resistance R .

By using Maxwell's equations together with (6)–(7), H_z^s and H_x^s can now be obtained easily for both $y > 0$ and $y < 0$. The spectral coefficients A_{\pm} and B_{\pm} , for $y \geq 0$, appearing in (6)–(7) are to be determined with the aid of the boundary conditions. To obtain a unique solution, it is also necessary to take into account the appropriate edge conditions as $x \rightarrow 0$, which were recently given by Idemen (2000) as $E_x = O(\ln x)$, $E_y = O(\ln x)$, $E_z = O(1)$ and $H_x = O(x^{-1/2})$, $H_y = O(x^{-1/2})$, $H_z = o(1)$. These conditions define the behavior of the electromagnetic field at the junction of a PEC half-plane and a resistive half-plane.

Now, by substituting the scattered field expressions into the boundary conditions and inverting, the resulting integral equations

$$\frac{2\alpha k_z}{\omega\mu\Gamma} A_+(\alpha) + \left[\frac{-2N^2}{\omega\mu\Gamma} + \frac{1}{R_1} \right] B_+(\alpha) = \Phi_1^t(\alpha) - \frac{h}{2\pi i(\alpha - k_x)}, \tag{10}$$

$$\left[\frac{-2(k^2 - \alpha^2)}{\omega\mu\Gamma} + \frac{1}{R_2} \right] A_+(\alpha) + \frac{2\alpha k_z}{\omega\mu\Gamma} B_+(\alpha) = \Phi_2^t(\alpha) - \frac{j}{2\pi i(\alpha - k_x)} \tag{11}$$

are obtained since $A_+(\alpha) = A_-(\alpha) = \Phi_1^U(\alpha)$ and $B_+(\alpha) = B_-(\alpha) = \Phi_2^U(\alpha)$. In the above expressions,

$$h = \frac{1}{k_y \omega\mu} \{ (-N^2 - k_y^2) A_x^i + k_x k_y A_y^i + k_x k_z A_z^i \} \tag{12}$$

and

$$j = \frac{1}{k_y \omega\mu} \{ k_x k_z A_x^i - k_y k_z A_y^i + (-2k_y^2 - k_z^2) A_z^i \}, \tag{13}$$

while $\Phi_{1,2}^U(\alpha)$ and $\Phi_{1,2}^L(\alpha)$ are yet unknown functions regular in the half-plane $Im(\alpha) > Im(k_x)$ and $Im(\alpha) < Im(N)$, respectively. The elimination of $A_{\pm}(\alpha)$

and $B_{\pm}(\alpha)$ gives a matrix Wiener-Hopf equation written in the strip $Im(k_x) < Im(\alpha) < Im(N)$ as follows:

$$\mathbf{G}(\alpha)\Phi^U(\alpha) = \Phi^L(\alpha) + \mathbf{V}(\alpha) \quad (14)$$

with

$$\mathbf{G}(\alpha) = \begin{bmatrix} \frac{2\alpha k_z}{\omega\mu\Gamma} & \frac{-2N^2}{\omega\mu\Gamma} + \frac{1}{R_1} \\ \frac{-2(k^2 - \alpha^2)}{\omega\mu\Gamma} + \frac{1}{R_2} & \frac{2\alpha k_z}{\omega\mu\Gamma} \end{bmatrix} \quad (15)$$

and

$$\mathbf{V}(\alpha) = [V_1, V_2]^T = \left[\frac{-h}{2\pi i(\alpha - k_x)}, \frac{-j}{2\pi i(\alpha - k_x)} \right]^T. \quad (16)$$

Here, the superscript T denotes the transpose of the matrix and $\Phi^U(\alpha)$, $\Phi^L(\alpha)$ and $\mathbf{V}(\alpha)$ are column vectors. The terms $\Phi^U(\alpha)$, $\Phi^L(\alpha)$ are unknown functions that need to be determined and $\mathbf{V}(\alpha)$ corresponds to the contributions of the incident and reflected fields as given in (16).

Factorization of the Kernel Matrix

The factorization of the kernel matrix for the present diffraction problem is accomplished by employing the Daniele-Khrapkov method (Büyükaksoy, & Serbest, 1993). Now, let the matrix $\mathbf{G}(\alpha)$, given by (15), be written as

$$\mathbf{G}(\alpha) = \mathbf{B}\tilde{\mathbf{G}}(\alpha), \quad (17)$$

yielding $\tilde{\mathbf{G}}(\alpha)$ in a form appropriate for Daniele-Khrapkov factorization with \mathbf{B} being a constant matrix

$$\mathbf{B} = \begin{bmatrix} 0 & 1/R_1 \\ 1/R_2 & 0 \end{bmatrix}$$

and

$$\tilde{\mathbf{G}}(\alpha) = a_1(\alpha)\mathbf{I} + a_2(\alpha) \begin{bmatrix} \ell_1(\alpha) & m(\alpha) \\ n(\alpha) & \ell_2(\alpha) \end{bmatrix}.$$

Here \mathbf{I} is the unit matrix and $a_1(\alpha) = 1$, $a_2(\alpha) = [\omega\mu\Gamma(\alpha)]^{-1}$, $n(\alpha) = 2\alpha k_z R_1$, $m(\alpha) = 2\alpha k_z R_2$, $\ell_1(\alpha) = -2R_2(k^2 - \alpha^2)$, $\ell_2(\alpha) = -2R_1 N^2$. Since \mathbf{B} is a scalar matrix, it is sufficient to consider only the factorization of $\tilde{\mathbf{G}}(\alpha)$. By adding and subtracting $s(\alpha)$, the trace of the matrix $\tilde{\mathbf{G}}(\alpha)$, it will be written as follows in Daniele-Khrapkov form:

$$\tilde{\mathbf{G}}(\alpha) = s(\alpha)\mathbf{I} + a_2(\alpha)\mathbf{J}(\alpha), \quad (18)$$

where

$$\mathbf{J}(\alpha) = \begin{bmatrix} \ell(\alpha) & m(\alpha) \\ n(\alpha) & -\ell(\alpha) \end{bmatrix}$$

with

$$s(\alpha) = 1 - [\omega\mu\Gamma(\alpha)]^{-1} \{R_2(k^2 - \alpha^2) + R_1N^2\}$$

and

$$\ell(\alpha) = R_1N^2 - R_2(k^2 - \alpha^2).$$

The eigenvalues of the matrix $\tilde{\mathbf{G}}(\alpha)$ are

$$\lambda_{1,2}(\alpha) = s(\alpha) \pm a_2(\alpha)\sqrt{f(\alpha)}, \quad (19)$$

where

$$f(\alpha) = [R_1N^2 - R_2(k^2 - \alpha^2)]^2 - 4R_1R_2\alpha^2k_z^2,$$

and from (19) the explicit expressions are obtained as

$$\lambda_{1,2}(\alpha) = 1 - [\omega\mu\Gamma(\alpha)]^{-1} \{R_2(k^2 - \alpha^2) + R_1N^2\} \\ \pm [\omega\mu\Gamma(\alpha)]^{-1} \sqrt{[R_1N^2 - R_2(k^2 - \alpha^2)]^2 + 4\alpha^2k_z^2R_1R_2}.$$

Now, instead of continuing the analysis for the general case, let us assume that $R_1R_2 \ll 1$, which will yield the following approximation:

$$4\alpha^2k_z^2R_1R_2 \ll [R_1N^2 - R_2(k^2 - \alpha^2)]^2,$$

and one can easily write

$$f(\alpha) = R_2^2(\alpha^2 - \alpha_1^2)^2 \quad \text{with} \quad \alpha_1^2 = -\frac{1}{R_2} [(R_1 - R_2)k^2 - R_1k_z^2]. \quad (20)$$

So, the eigenvalues will be reduced to

$$\lambda_1(\alpha) = 1 - 2R_2(k^2 - \alpha^2)[\omega\mu\Gamma(\alpha)]^{-1} \quad (21)$$

and

$$\lambda_2(\alpha) = 1 - 2R_1N^2[\omega\mu\Gamma(\alpha)]^{-1}. \quad (22)$$

The first step of the solution requires the factorization of these eigenvalues as a product of upper and lower split functions. For this purpose, let the eigenvalue in (21) be written by simple manipulations as

$$\lambda_1(\alpha) = -\frac{2R_2}{kZ_0} \cot^2 \theta_0 \cdot \frac{\Gamma(\alpha)}{\chi(\xi_1, \alpha)\chi(\xi_2, \alpha)}, \quad (23)$$

where

$$\xi_{1,2} = (-\sin \theta_0) / \{(-Z_0/4R_2) \pm \sqrt{(Z_0/R_2)^2 - \cos^2 \theta_0}\}.$$

The function $\chi(\xi, \alpha)$ given in (23) is defined as

$$\chi(\xi, \alpha) = \frac{\Gamma(\alpha)}{N + \xi\Gamma(\alpha)} = \chi^U(\xi, \alpha)\chi^L(\xi, \alpha),$$

which is factorized in terms of Maliuzhinetz function (see Uzgören, Büyükaksoy, & Serbest, 1989) so that the factors of $\lambda_1(\alpha)$ are

$$\lambda_1^{U,L}(\alpha) = \sqrt{-\frac{2R_2}{kZ_0} \cot \theta_0} \cdot \frac{\sqrt{N \pm \alpha}}{\chi^{U,L}(\xi_1, \alpha)\chi^{U,L}(\xi_2, \alpha)}.$$

In the same manner, $\lambda_2(\alpha)$ can be written as

$$\lambda_2(\alpha) = -2(R_1/Z_0) \sin \theta_0 \chi^{-1}(\xi, \alpha),$$

and also the factors of $\lambda_2(\alpha)$ can easily be obtained as

$$\lambda_2^{U,L}(\alpha) = [-2(R_1/Z_0) \sin \theta_0]^{1/2} [\chi^{U,L}(\xi, \alpha)]^{-1}.$$

Since $f(\alpha)$ appearing in (19) is a fourth-order polynomial, it is obvious that the factor matrices will have an exponential behavior. The next step is, therefore, to introduce a polynomial matrix in the form given by Daniele (1984) to cancel this exponential growth. As known, the order of this polynomial matrix will be of the order of \sqrt{f} , and since it is a second-order polynomial for the problem under consideration, it will involve only one unknown coefficient to be determined with the aid of the regularity condition. So, the polynomial matrix $\mathbf{P}(\alpha)$ can be taken as

$$\mathbf{P}(\alpha) = -R_2(\alpha^2 + \beta^2)\mathbf{I} + \mathbf{J}(\alpha) \quad (24)$$

and the eigenvalues of $\mathbf{P}(\alpha)$ are

$$\lambda_{p1,p2}(\alpha) = -R_2(\alpha^2 + \beta^2) \pm \sqrt{f(\alpha)} \quad (25)$$

with $\lambda_{p1}(\alpha)\lambda_{p2}(\alpha) = 2R_2^2(\beta^2 + \alpha_1^2)(\alpha^2 - \alpha_0^2)$, where $\alpha_0^2 = (\alpha_1^4 - \beta^4)/2(\beta^2 + \alpha_1^2)$ and α_1^2 is given by (20). The second step is to split the eigenvalues of the polynomial matrix given in (25) as $\lambda_{p1}(\alpha) = r_1$ and $\lambda_{p2}(\alpha) = r_2\alpha^2 + r_3$, where $r_1 = R_1(k^2 - k_-^2) - R_2(k^2 + \beta^2)$, $r_2 = -2R_2$, and $r_3 = R_2(k^2 - \beta^2) - R_1(k^2 - k_-^2)$.

Also, the factors of the eigenvalues can easily be obtained by taking the square root of r_1 for λ_{p1} and factorizing the simple polynomial for λ_{p2} yield $\lambda_{p1}^{U,L}(\alpha) = \sqrt{r_1}$ and $\lambda_{p2}(\alpha) = (\sqrt{r_2}\alpha + i\sqrt{r_3})(\sqrt{r_2}\alpha - i\sqrt{r_3})$. Note that for the factors of the $\lambda_{p2}(\alpha)$, the numerical calculation of the constant β^2 will define which factor of $\lambda_{p2}(\alpha)$ is regular in the upper or lower half of the complex α -plane. The condition for determining β^2 is the regularity condition given as $E = E_p$, where

$$E = \frac{1}{2} \int_{-\infty}^{\infty} \frac{1}{\sqrt{f(t)}} \ln \frac{\lambda_1(t)}{\lambda_2(t)} dt$$

and

$$E_p = \frac{1}{2} \int_{-\infty}^{\infty} \frac{1}{\sqrt{f(t)}} \ln \frac{\lambda_{p1}(t)}{\lambda_{p2}(t)} dt.$$

The integral E can be evaluated in terms of known functions, and E_p can be expressed as an elliptic integral of the first kind (Hurd & Lüneburg, 1985). Then the condition $E = E_p$ translates into

$$\alpha_0 = \alpha_1 ns \left(\frac{i\alpha_1 R_2}{\pi} E \right),$$

where $ns(x) = 1/\text{sn}(x)$ and $\text{sn}(x)$ is the elliptic function. For any set of parameters, the integral E can be evaluated numerically and used to calculate α_0 and consequently β . Now, the formal expressions of the factor matrices can be written as

$$\begin{aligned} \mathbf{G}_L(\alpha) &= \sqrt{\frac{\lambda_{1L}\lambda_{2L}}{\lambda_{p1L}\lambda_{p2L}}} \begin{bmatrix} 0 & 1/R_1 \\ 1/R_2 & 0 \end{bmatrix} \\ &\times \left\{ \begin{bmatrix} 1 & 0 \\ 0 & 1 \end{bmatrix} \cosh \left[\frac{1}{2} \ln \frac{\lambda_{1L}\lambda_{p2L}}{\lambda_{2L}\lambda_{p1L}} \right] + \frac{1}{\sqrt{f}} \begin{bmatrix} \ell & m \\ n & -\ell \end{bmatrix} \sinh \left[\frac{1}{2} \ln \frac{\lambda_{1L}\lambda_{p2L}}{\lambda_{2L}\lambda_{p1L}} \right] \right\} \mathbf{P}_L(\alpha), \end{aligned}$$

$$\begin{aligned} \mathbf{G}_U(\alpha) &= \sqrt{\frac{\lambda_{1U}\lambda_{2U}}{\lambda_{p1U}\lambda_{p2U}}} \mathbf{P}_U(\alpha) \\ &\times \left\{ \begin{bmatrix} 1 & 0 \\ 0 & 1 \end{bmatrix} \cosh \left[\frac{1}{2} \ln \frac{\lambda_{1U}\lambda_{p2U}}{\lambda_{2U}\lambda_{p1U}} \right] + \frac{1}{\sqrt{f}} \begin{bmatrix} \ell & m \\ n & -\ell \end{bmatrix} \sinh \left[\frac{1}{2} \ln \frac{\lambda_{1U}\lambda_{p2U}}{\lambda_{2U}\lambda_{p1U}} \right] \right\}. \end{aligned}$$

Here, the factorization of the polynomial matrix

$$\mathbf{P}(\alpha) = \begin{bmatrix} a & b\alpha \\ c\alpha & d\alpha^2 + e \end{bmatrix} = \mathbf{P}_U(\alpha) \mathbf{P}_L(\alpha)$$

is obtained with

$$\mathbf{P}_U(\alpha) = \begin{bmatrix} \sqrt{a} & 0 \\ c\alpha/\sqrt{a} & S(\alpha + \alpha_0)/\sqrt{a} \end{bmatrix}$$

and

$$\mathbf{P}_L(\alpha) = \begin{bmatrix} \sqrt{a} & b\alpha/\sqrt{a} \\ 0 & S(\alpha - \alpha_0)/\sqrt{a} \end{bmatrix}.$$

Here

$$S^2 = ad - bc = -ae/\alpha_0^2$$

is given with $a = R_1(k^2 - k_+^2) - R_2(k^2 + \beta^2)$, $b = 2k_-R_2$, $c = 2k_-R_1$, $d = -2R_2$, $e = R_2(k^2 - \beta^2) - R_1(k^2 - k_+^2)$. Now, this completes the factorization of the kernel matrix yielding a rigorous solution for the matrix Wiener-Hopf problem.

Note that if the approximation shown in (20) is not done, it would be impossible to obtain explicit expressions for the upper and lower functions which appear in the formal solution.

Analysis of the Diffracted Field

The analysis of the scattered field requires one to know the spectral coefficients $A_{\pm}(\alpha)$ and $B_{\pm}(\alpha)$ appearing in (6)–(7). It is sufficient to determine these spectral coefficients if $\phi_1^U(\alpha)$ and $\phi_2^U(\alpha)$ are known. Since the kernel matrix of the Wiener–Hopf problem is factorized, the formal solution can easily be written by following the standard procedure

$$\Phi_U(\alpha) = \frac{1}{2\pi i} \frac{1}{(\alpha - k_x)} [\mathbf{G}_U(\alpha)]^{-1} [\mathbf{G}_L(k_x)]^{-1} [-h, -j]^T.$$

The diffracted field will be obtained by the steepest descent method after writing the spectral coefficients in terms of the upper regular functions.

In this section, four different special cases involving extreme, but practically meaningful, resistance values are considered. One of the resistances on the $x > 0$ part of the plane is taken to be either zero or infinite, while the other is kept finite and nonzero. For example, R_1 or R_2 is taken as infinite, while the other is kept finite and R_1 or R_2 is taken as zero while the other is again kept finite and different than zero. Each of these problems is formulated into a pair of simultaneous Wiener–Hopf equations that are decoupled via a polynomial transformation and solved through the standard procedure, where the field expressions are derived in geometrical theory of diffraction (GTD) form. In the following, only the essential steps of the solution will be shown by omitting the intermediate ones, and diffraction coefficients will be given for each case.

Case for $R_1 \rightarrow \infty$ or $R_2 \rightarrow \infty$

R_1 and R_2 are the resistances along the x -axis and the z -axis, respectively, on the $x > 0$ part of the Oxz -plane. If R_1 or R_2 is infinitely large, the physical body along the corresponding axis on the $x > 0$ part of the plane will vanish. This will yield a PEC half-plane along this axis on the $x < 0$ part of the plane, leaving a resistance discontinuity along the other axes of the plane.

Now, when R_2 is taken to be infinitely large, it reduces the configuration into two separate problems: a PEC half-plane along the z -axis and a resistance discontinuity along the x -axis (Figure 3a). As a result of this approximation, the original problem given by (10)–(11) yields two simultaneous Wiener–Hopf equations:

$$\frac{2\alpha k_z}{\omega\mu\Gamma(\alpha)} \Phi_1^U + \left[-\frac{2N^2}{\omega\mu\Gamma(\alpha)} + \frac{1}{R_1} \right] \Phi_2^U = \Phi_1^L + V_1 \quad (26)$$

and

$$[\omega\mu\Gamma(\alpha)]^{-1} [-2(k^2 - \alpha^2)\Phi_1^U + 2\alpha k_z \Phi_2^U] = \Phi_2^L + V_2. \quad (27)$$

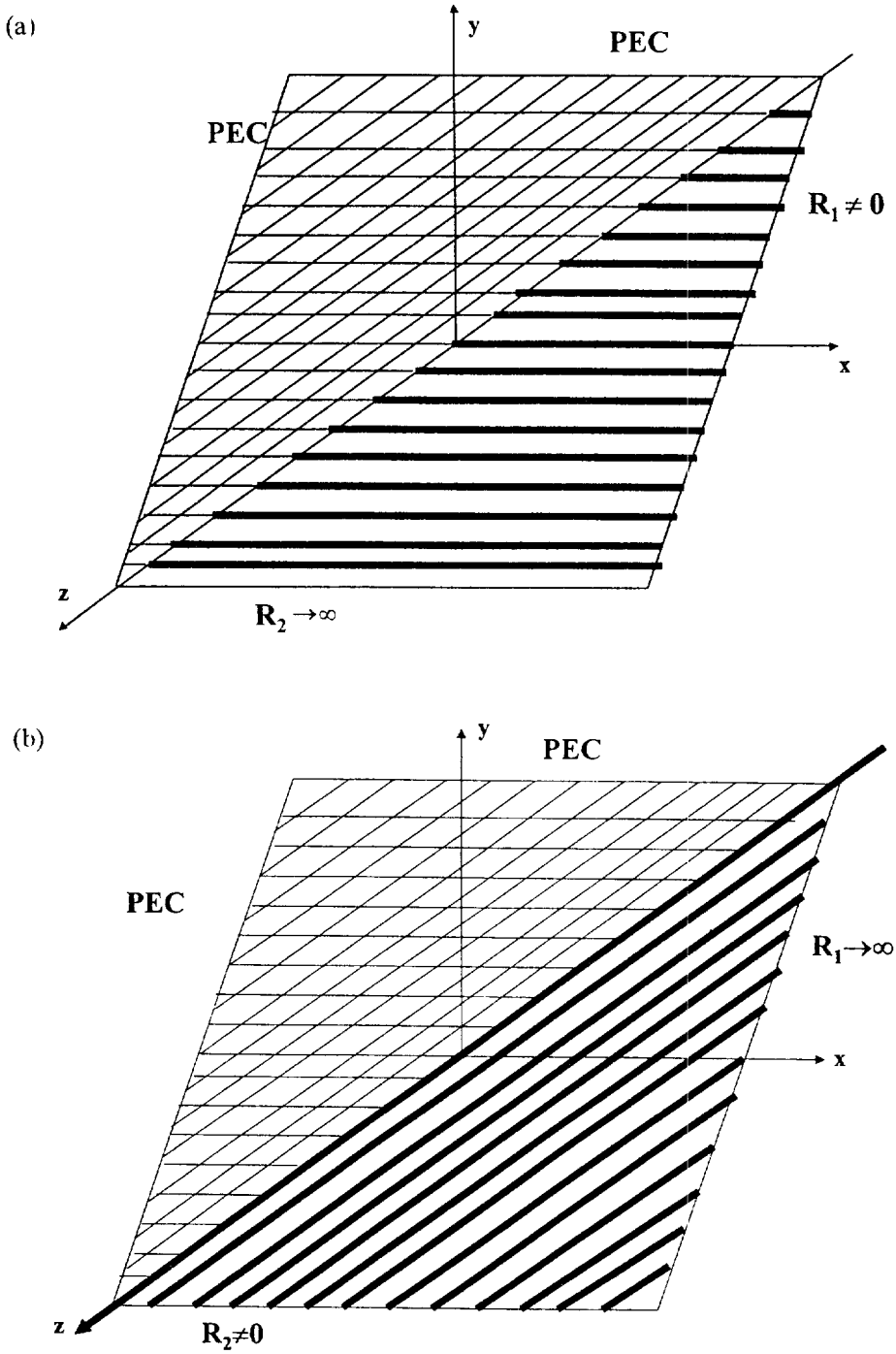


Figure 3. (a) Case $R_2 \rightarrow \infty$: PEC half-plane and resistance discontinuity along x -axis. (b) Case $R_1 \rightarrow \infty$: PEC half-plane and resistance discontinuity along z -axis.

Since both Φ_1^U and Φ_2^U are regular functions in the upper half-plane, the combination of these two functions in (27) is also regular in the upper half-plane. Here, V_1 and V_2 denote the elements of the column matrix $\mathbf{V}(\alpha)$ given by (16).

Let

$$\Psi^U(\alpha) = -2(k^2 - \alpha^2)\Phi_1^U + 2\alpha k_z \Phi_2^U, \tag{28}$$

so that (27) is reduced into the form

$$[\omega\mu\Gamma(\alpha)]^{-1}\Psi^U(\alpha) = \Phi_2^L + V_2.$$

As is seen, the polynomial transformation given in (28) reduced the simultaneous system of equations in (26)–(27) into two scalar Wiener–Hopf equations. Therefore, (27) will be solved first, to express Φ_1^U in terms of Φ_2^U . Then, (26) will also be reduced to a scalar equation involving only Φ_2^U and Φ_1^L . Then, performing the standard Wiener–Hopf decomposition procedure, one obtains the solution as follows:

$$\begin{aligned} \Phi_2^U = & \frac{\sin^2 \theta_0}{2\pi i \cos^2 \theta_0} \left\{ hR_1 \frac{(k - k_x)(k + \alpha)}{(N - k_x)(N + \alpha)(\alpha - k_x)} - j\sqrt{R_1} k_x k_z \right. \\ & \left. \times \frac{(k + \alpha)}{(\alpha - k_x)(k + k_x)(N + \alpha)(N - k_x)} \right\} \chi^L(\xi_1, k_x) \chi^L(\xi_2, k_x) \chi^U(\xi_1, \alpha) \chi^U(\xi_2, \alpha). \end{aligned} \tag{29}$$

The function $\chi(\xi, \alpha)$ in (29) has the same form as the function appearing in (23), which is factorized in terms of Maliuzhinetz function (Uzgören, Büyükaksoy, & Serbest, 1989). Here, $\xi_{1,2}$ denote

$$\xi_{1,2} = (Z_0 \sin \theta_0) / [(-R_1) \pm \sqrt{R_1^2 - (Z_0 \cos \theta_0)^2}]^{-1}.$$

Since Φ_1^U was expressed in terms of Ψ^U and Φ_2^U in (28), one can obtain the following formula for Φ_1^U :

$$\Phi_1^U = j \frac{kZ_0 \sqrt{N - k_x} \sqrt{N + \alpha}}{4\pi i (\alpha - k_x)(k^2 - \alpha^2)} + \frac{\alpha k_z}{(k^2 - \alpha^2)} \Phi_2^U.$$

Now, using the expressions of the spectral coefficients, the diffracted fields can be obtained by using steepest descent method, yielding the diffraction coefficients as

$$\begin{aligned} D_x(\theta_0, \phi_0, \phi) = & \frac{e^{-i\pi/4} R_1 \chi^U(\xi_1, -N \cos \phi) \chi^U(\xi_2, -N \cos \phi)}{i\sqrt{2\pi} Z_0 (1 - \cos \phi)(1 - \cos \phi_0)} \\ & \times \frac{\chi^L(\xi_1, N \cos \phi_0) \chi^L(\xi_2, N \cos \phi_0) (1 - \sin \theta_0 \cos \phi) \sin \phi}{(\cos \phi + \cos \phi_0) \cos \phi_0} Y \end{aligned} \tag{30}$$

and

$$D_z(\theta_0, \phi_0, \phi) = -\frac{e^{-i\pi/4} \sin \phi \sqrt{1 - \cos \phi_0}}{i2\sqrt{2\pi} \sin \phi_0 (\cos \phi + \cos \phi_0)} \cdot \frac{\sqrt{1 - \cos \phi}}{(1 - \sin^2 \theta_0 \cos^2 \phi)} \\ \times \left\{ -\cos \theta_0 (\cos \theta_0 - \sin \theta_0 \cos \phi_0) - \sin \theta_0 \sin \phi_0 (2 \sin \theta_0 \sin \phi_0 + \cos \theta_0) \right\} \\ - \frac{\sin \theta_0 \cos \phi \cos \theta_0}{1 - \sin^2 \theta_0 \cos^2 \phi} D_x(\theta_0, \phi_0, \phi), \quad (31)$$

with

$$Y = \frac{(1 - \sin \theta_0 \cos \phi_0)}{\cos \theta_0 \sin \phi_0} \cdot \left\{ -\sin \theta_0 (1 + \sin^2 \phi_0) + \cos \phi_0 (\sin \theta_0 \sin \phi_0 + \cos \theta_0) \right\} \\ + \left\{ -\cos \theta_0 (\cos \theta_0 - \sin \theta_0 \cos \phi_0) - \sin \theta_0 \sin \phi_0 (2 \sin \theta_0 \sin \phi_0 + \cos \theta_0) \right\} \\ \times \frac{\cos \phi_0}{(1 + \sin \theta_0 \cos \phi_0) \sin \theta_0 \sin \phi_0}.$$

Now, similar to the previous case, the approximation for $R_1 \rightarrow \infty$ (Figure 3b) yields a PEC half-plane along the $x > 0$ part of the x -axis and a resistance discontinuity along the z -axis. The diffraction coefficients are obtained in this case as

$$D_z(\theta_0, \phi_0, \phi) = -\frac{e^{-i\pi/4} R_2 \sin \phi}{i\sqrt{2\pi} Z_0 \sqrt{(1 - \cos \phi) \sin \theta_0}} \frac{\chi^U(\xi, -N \cos \phi) \chi^U(\xi, -N \cos \phi_0)}{(\cos \phi + \cos \phi_0) \sqrt{1 - \cos \phi_0}} \\ \times \left\{ -2 \sin^2 \theta_0 \sin \phi_0 - \sin \phi_0 - \sin \theta_0 \cos \theta_0 \sin^2 \phi_0 - \sin \theta_0 \cos \theta_0 \sin \phi_0 \cos \phi_0 \right\} \quad (32)$$

and

$$D_x(\theta_0, \phi_0, \phi) = -\frac{e^{-i\pi/4} \sqrt{1 - \cos \phi_0} \sqrt{1 - \cos \phi} \sin \phi}{i2\sqrt{2\pi} \sin \theta_0 (\cos \phi + \cos \phi_0) \sin \phi_0} \\ \times \left\{ -\sin \theta_0 - \sin \theta_0 \sin^2 \phi_0 + \sin \theta_0 \sin \phi_0 \cos \phi_0 + \cos \phi_0 \cos \theta_0 \right\} \\ - \frac{\cos \phi \cos \theta_0}{\sin^2 \theta_0} D_z(\theta_0, \phi_0, \phi), \quad (33)$$

with $\xi = (-2R_2/Z_0 \sin \theta_0)$, where the function $\chi(\xi, \alpha)$ has the same form as in (23).

Case for $R_1 = 0$, $R_2 \neq 0$ or $R_2 = 0$, $R_1 \neq 0$

As is obvious, a vanishing surface resistance corresponds to a perfectly conducting structure. So, when R_1 or R_2 is equal to zero, it yields a PEC full plane along that axis and gives a resistance discontinuity along the other axis.

Now, letting $R_1 \rightarrow 0$ (Figure 4a), the following can easily be obtained:

$$\left[\frac{-2(k^2 - \alpha^2)}{\omega \mu \Gamma(\alpha)} + \frac{1}{R_2} \right] \Phi_1^U = \Phi_2^L + V_2, \quad \text{Im}\{k_x\} < \text{Im}\{\alpha\} < \text{Im}\{N\} \quad (34)$$

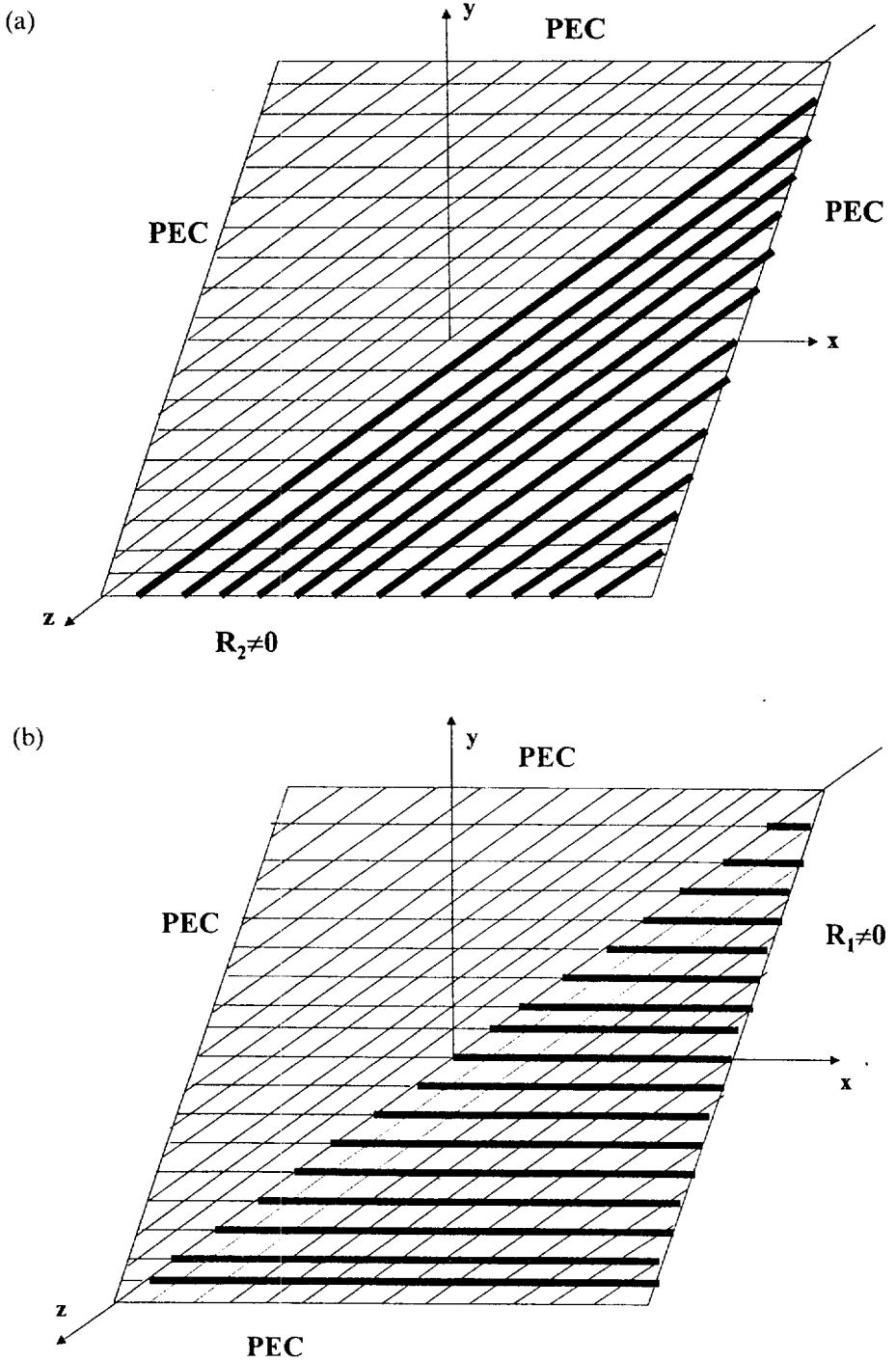


Figure 4. (a) Case $R_1 = 0$: PEC full-plane and resistance discontinuity along z -axis. (b) Case $R_2 = 0$: PEC full-plane and resistance discontinuity along x -axis.

with $\Phi_2^U = 0$, $B_{\pm}(\alpha) = 0$ and $E_x^s = E_x^r = -A_x^i \exp(-ik_x x + ik_y y)$. Wiener-Hopf factorization gives

$$\Phi_1^U(\alpha) = j \frac{kZ_0}{4\pi i} \tan^2 \theta_0 \frac{\chi^L(\xi_1, k_x) \chi^L(\xi_2, k_x)}{\sqrt{N - k_x}} \cdot \frac{\chi^U(\xi_1, \alpha) \chi^U(\xi_2, \alpha)}{\sqrt{N + \alpha(\alpha - k_x)}}$$

and the diffraction coefficient is obtained as

$$D_{\pm}^d(\theta_0, \phi_0, \phi) = - \frac{e^{-i\pi/4}}{i2\sqrt{2\pi}} \cdot \frac{\sin \phi (\cos^2 \theta_0 \sin \phi_0)^{-1}}{\sqrt{1 - \cos \phi} \sqrt{1 - \cos \phi_0} (\cos \phi + \cos \phi_0)}$$

$$\times \{ \chi^U(\xi_1, -N \cos \phi) \chi^U(\xi_2, -N \cos \phi) \chi^L(\xi_1, N \cos \phi_0) \chi^L(\xi_2, N \cos \phi_0) \}$$

$$\times \{ -2 \sin^2 \theta_0 \sin^2 \phi_0 - \cos^2 \theta_0 + \sin \theta_0 \cos \theta_0 \cos \phi_0 - \sin \theta_0 \cos \theta_0 \sin \phi_0 \}$$
(35)

with

$$\xi_{1,2} = (4R_2 \sin \theta_0) \left/ \left[Z_0 \mp \sqrt{Z_0^2 - (4R_2 \cos \theta_0)^2} \right] \right.$$

On the other hand, by letting $R_2 \rightarrow 0$ (Figure 4b), the following equation is obtained:

$$-\frac{2N}{kZ_0} [\chi(\xi, \alpha)]^{-1} \Phi_{\pm}^U = \Phi_1^L - \frac{h}{2\pi i(\alpha - k_x)}, \quad \text{Im}\{k_x\} < \text{Im}\{\alpha\} < \text{Im}\{N\} \quad (36)$$

with $\xi = -kZ_0/2R_1N$. Then, after performing the Wiener-Hopf factorization, the diffraction coefficient is obtained as

$$D_x^d(\theta_0, \phi_0, \phi) = \frac{e^{-i\pi/4}}{2\sqrt{2\pi}i} \cdot \frac{\sin \phi}{(\cos \phi + \cos \phi_0)} \chi^U(\xi, -N \cos \phi) \chi^U(\xi, -N \cos \phi_0)$$

$$\times \frac{1}{\sin \theta_0 \sin \phi_0} \{ \sin \theta_0 + \sin \theta_0 \sin^2 \phi_0 - \sin \theta_0 \sin \phi_0 \cos \phi_0 - \cos \theta_0 \cos \phi_0 \}.$$
(37)

Numerical Results and Concluding Remarks

Some numerical results have been obtained for the diffracted fields where the ambient medium is taken as free space and the incident plane wave electric field strength is assumed to be 1 V/m. The diffracted field expressions involve the split functions $\chi^{U,L}(\alpha)$, which are written in terms of the Maliuzhinetz function, as was done by Uzgören, Büyükkaksoy, Serbest, 1989. Then, the Maliuzhinetz function is easily computed by using the approximate formulas given by Volakis and Senior (1985).

Figures 5 and 6 illustrate the variation of the amplitude of the x- and z-components of $20 \log_{10}(|u_d|/\sqrt{N\rho})$ with respect to the observation angle for various values of the normalized resistance (R/Z_0). The diffracted field expressions obtained here are not uniform and, consequently, it is expected that the field will take very

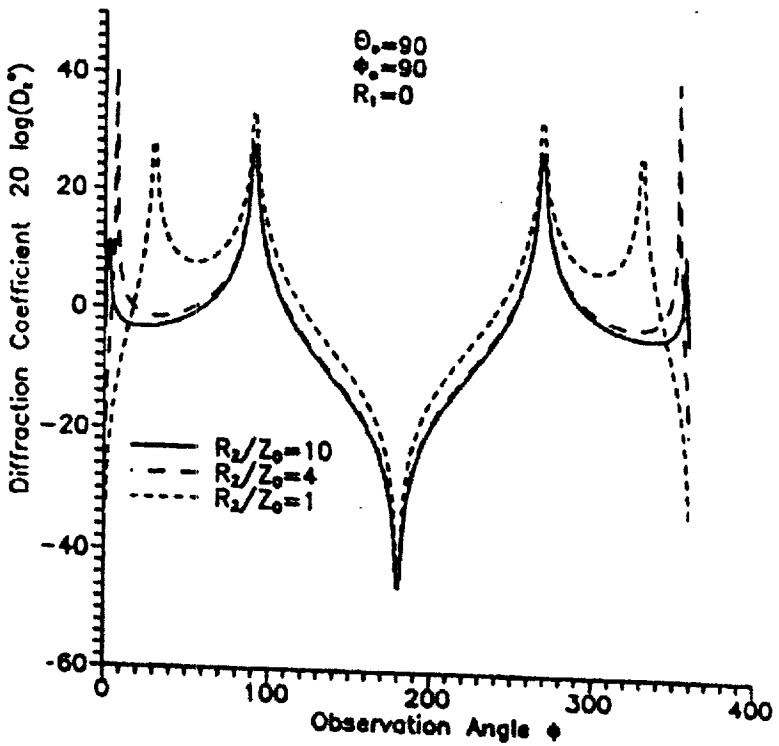
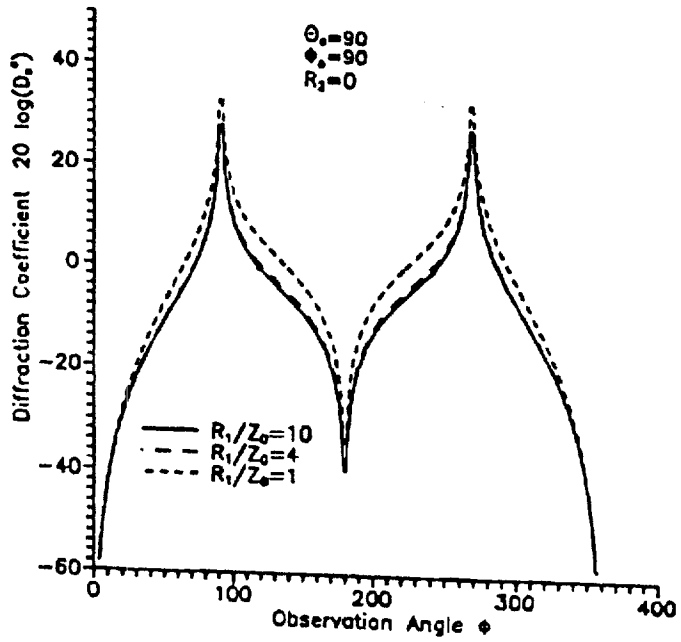


Figure 5. Variation of the diffraction coefficient for $\theta_0 = \phi_0 = \pi/2$: (a) D_x for $R_2 = 0$ and (b) D_z for $R_1 = 0$.

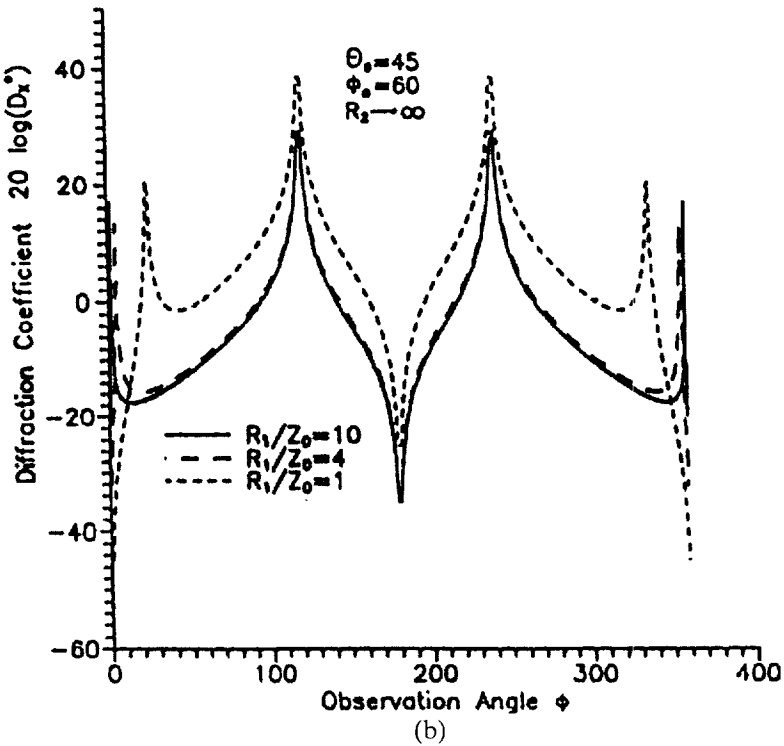
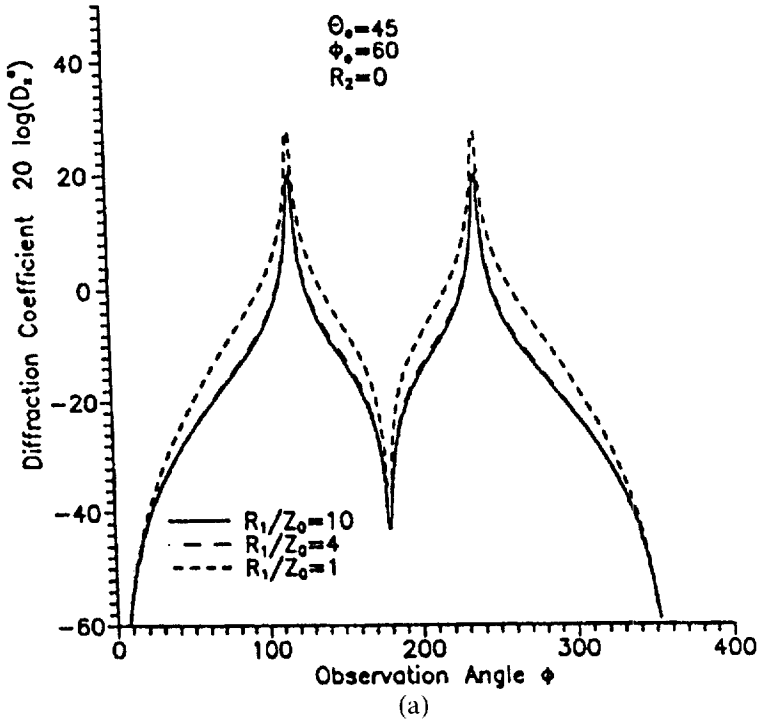


Figure 6. Variation of the diffraction coefficient for $\theta_0 = 45$, $\phi_0 = 60$: (a) D_x for $R_2 = 0$, (b) D_x for $R_2 \rightarrow \infty$, (c) D_x for $R_1 \rightarrow \infty$.

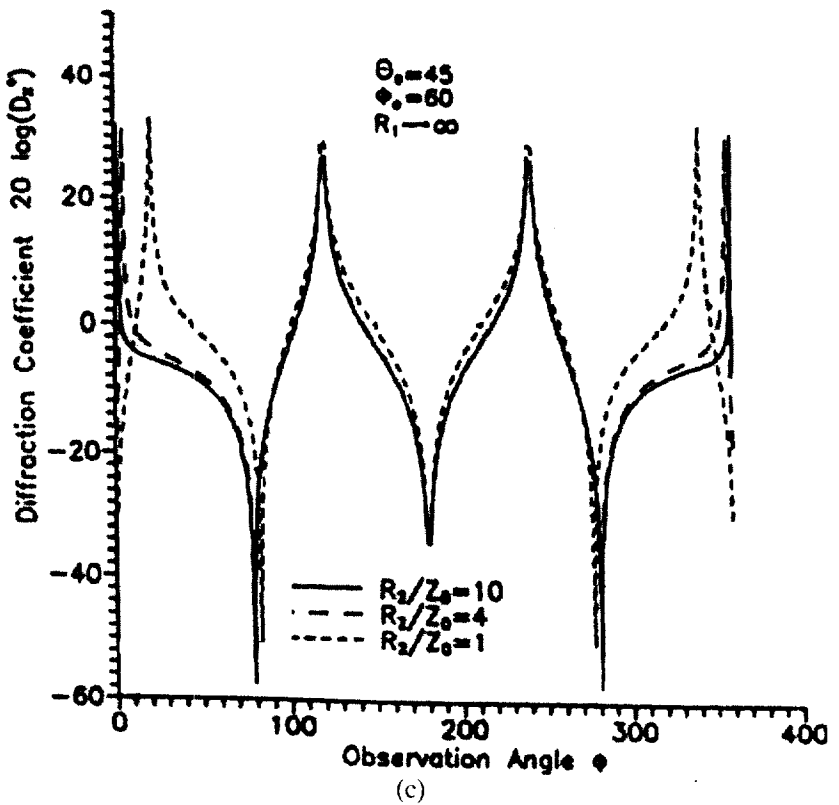


Figure 6. Continued.

large values in the transition regions. As is seen from the figures and also from the analytical expressions, the transition boundaries are determined by the incidence angle as $(\pi - \phi_0)$ and $(\pi + \phi_0)$.

Figures 5a and 5b show the variation of the diffraction coefficients for the normal incidence case, i.e., $\theta_0 = \phi_0 = \pi/2$. In Figure 5a, the behavior of D_x is shown for resistance discontinuity along the z -axis over a PEC full plane ($R_2 = 0$). It should be noted that the behavior of D_x is the same for the resistance discontinuity over a PEC half-plane located at the negative part of the x -axis ($R_2 \rightarrow \infty$). Also, Figure 5b shows the diffraction coefficient D_z for $R_1 = 0$ (PEC full plane along the x -axis), which has the same variation for $R_1 \rightarrow \infty$, again corresponding to a PEC half-plane located along the negative half of the x -axis. This result is not surprising because no mutual effects are expected in the normal incidence case.

The variation of the diffraction coefficient D_x with respect to the observation angle is given in Figures 6a–6c for the incidence angles $\theta_0 = 45$, $\phi_0 = 60$. Figure 6a shows D_x for $R_2 = 0$, and it has been obtained that D_z for $R_1 = 0$ have almost the same behavior for all R/Z_0 values. The form of the variation of the diffraction coefficients D_x for $R_2 \rightarrow \infty$ (Figure 6b) and D_z for $R_1 \rightarrow \infty$ are also the same, but the magnitudes of the maximum and minimum points are different. Similarly, D_x for $R_1 \rightarrow \infty$ (Figure 6c) and D_z for $R_2 \rightarrow \infty$ have the same behavior. This consideration is repeated for the cases in which the incidence angles are $\theta_0 = 30$,

$\phi_0 = 20$ and $\theta_0 = 65$, $\phi_0 = 140$ and the relations between the diffraction coefficients for all cases are observed to be the same. In contrast to the normal incidence case, mutual effects are of considerable importance for oblique incidence. Also, these graphs show that the diffraction coefficients D_x and D_z corresponding to a resistance discontinuity on either a PEC full plane or a PEC half-plane have the same behavior with respect to the observation angle.

It should be noted that the problem of diffraction from a discontinuity formed by a PEC half-plane and an anisotropic resistive half-plane is considered for the first time in this work. Although there are studies about anisotropic conducting structures which already appeared in the open literature (as in Hurd, 1960, and [Eüyükaksoy, Serbest, Kara, 1996; Rozov, Tretyakov, 1981, 1984]), they involve semi-infinite geometries, and it is not possible to reduce the geometrical configuration considered in this work to a half-plane with anisotropic conductivity. Therefore, there has been no opportunity to compare the results presented here with some previously obtained results to validate the accuracy of the present high-frequency solution. But both the analytical expressions and the numerical results are in agreement with the expectations related to the problem, and these points are explained above.

Finally, some additional remarks will be made that may be considered as a verification of the solution presented here, even though they are necessary but not sufficient conditions to establish the accuracy of the solution. In the normal incidence case ($\theta_0 = \pi/2$) for both $R_1 \rightarrow \infty$ and $R_2 \rightarrow \infty$ the z -component of the diffracted electric field reduces in the E_z polarization case to the following well-known result for the PEC half-plane problem:

$$E_z^d = -\frac{e^{j\pi/4}}{\sqrt{2\pi}} \frac{\sqrt{1 + \cos \phi_0} \sqrt{1 + \cos \phi}}{\cos \phi + \cos \phi_0} \cdot \frac{e^{jk\rho}}{\sqrt{k\rho}}$$

On the other hand, analytical results yield $D_x = 0$ for $R_1 = 0$ and $D_z = 0$ for $R_2 = 0$ at all incidence angles. Therefore, the z -component and x -component of the scattered field, respectively, involve only the reflected term as expected.

References

- Büyükaksoy, A., & A. H. Serbest. 1993. Matrix Wiener-Hopf factorization methods and applications to some diffraction problems. In *Analytical and numerical methods in electromagnetic wave theory*, M. Hashimoto, M. Idemen & O. A. Tretyakov, eds., 257–315, Science House Co. Ltd. Tokyo.
- Büyükaksoy, A., A. H. Serbest, & A. Kara. 1996. Diffraction coefficient for a half-plane with anisotropic conductivity. *IEE Proc.-Sci. Meas. Technol.* 143(6):384–388.
- Daniele, V. G. 1984. On the solution of vector Wiener-Hopf equations occurring in scattering problems. *Radio Science* 19(5):1173–1178.
- Hurd, R. A. 1960. Diffraction by a unidirectionally conducting half-plane. *Canad. J. Phys.* 38:168–175.
- Hurd, R. A., & E. Lüneburg. 1985. Diffraction by an anisotropic impedance half-plane. *Canad. J. Phys.* 63:1135–1140.
- Idemen, M. 2000. Confluent edge conditions for the electromagnetic wave at the edge of a wedge bounded by material sheets. *Wave Motion* 32:37–55.
- Rozov, V. A., & A. A. Sochava. 1991. Diffraction of electromagnetic waves by a semi-infinite grid with square cells. *Radiophysics and Quantum Electronics* 34(5):490–496.

- zov, V. A., & S. A. Tretyakov. 1981. Diffraction of plane electromagnetic waves by a semi-infinite grid of parallel conductors. *Radioengineering and Electronic Physics* 26(11):6-15.
- zov, V. A., & S. A. Tretyakov. 1984. Diffraction of plane electromagnetic waves by a semi-infinite grid made of parallel conductors arranged at an angle to the grid's edge. *Radioengineering and Electronic Physics* 29(5):37-47.
- ior, T. B. A. 1978. Some problems involving imperfect half planes. In *Electromagnetic scattering*, ed. L. E. Uslenghi, 185-219. New York: Academic Press.
- best, A. H. 1997. Recent analytical developments in diffraction theory. In *Modern mathematical methods in diffraction theory and its applications in engineering*, ed. E. Mesiter, 203-217, Peter Lang GmbH: Frankfurt.
- best, A. H., & A. Büyükaksoy, & G. Uzgören. 1991. Diffraction at a discontinuity formed by two anisotropic impedance half-planes. *IEICE Transactions* E74(5):1283-1287.
- ören, G., A. Büyükaksoy, & A. H. Serbest. 1989. Diffraction coefficient related to a discontinuity formed by impedance and resistive halfplanes. *IEE Proceedings* 136, Pt. H, No. 1, 19-23.
- akis, J. L., & T. B. A. Senior. 1985. Simple expressions for a function occurring in diffraction theory. *IEEE Trans. Antennas Propagat.* AP-33:678-680.